

1 **Parametric study and speciation analysis of rare earth precipitation using** 2 **oxalic acid in a chloride solution system**

3 Ahmad Nawab, Xinbo Yang*, Rick Honaker

4 Department of Mining Engineering, University of Kentucky, Lexington, Kentucky 40506

6 ABSTRACT

7 Oxalic acid precipitation is a common step in the purification of rare earth elements (REE)
8 from a concentrated pregnant leach solution (PLS). However, the presence of contaminants such
9 as Al, Fe, and Ca in given amounts decreases the REE precipitation efficiency and product purity
10 while also increasing the amount of oxalic acid needed to maximize recovery. As such, a
11 statistically designed test program was performed to identify the optimal conditions necessary for
12 a relatively low REE content PLS containing elevated concentrations of contaminant ions. The
13 performance objective was maximization of REE precipitation efficiency while minimizing the
14 oxalic acid dosage. A central composite design was utilized to quantify performance impacts and
15 identify the ultimate set of parameter values for oxalic acid dosage, Fe(III) contamination
16 concentration, solution pH, and reaction temperature. The resultant model suggested that oxalic
17 acid dosage and reaction pH are the most significant factors for the REE precipitation efficiency,
18 followed by the interaction of oxalic dosage and Fe concentration. Test results indicate that
19 increasing the oxalic acid concentration from 0g/L to 80g/L improved the REE precipitation
20 efficiency from approximately 4.2% to 95.0%. Furthermore, raising the solution pH from 0.5 to
21 2.5 considerably enhanced the precipitation efficiency from 0.0% to 98.9%. A solution
22 temperature elevation decreased REE recovery, which indicated an exothermic reaction between
23 REEs and oxalate anions. Finally, a high level of Fe contamination adversely impacted REE
24 precipitation efficiency. To further the understanding of the REE-oxalate system, a fundamental
25 solution chemistry study was performed using the equilibrium constants of the reactions. The study
26 resulted in the development of oxalate speciation diagrams and provided an analysis of the REE
27 precipitation characteristics at various oxalate anion concentrations and Fe contamination levels
28 using MINTEQ software. The dominant iron species in the solution system were found to be Fe-
29 $(C_2O_4)_3^{3-}$, Fe- $(C_2O_4)^{2-}$, and Fe- $(C_2O_4)^+$, which consume the majority of the oxalate anions. The
30 simulated model was found to be in agreement with the experimental findings and helped to
31 explain the adverse impact of increased iron concentrations on REE precipitation efficiency.

32 **Keywords:** Rare earth elements, selective precipitation, oxalic acid, purification, process
33 optimization, contaminant elements

1. Introduction

Rare earth elements (REE) are a group of 17 elements, including scandium (Sc), yttrium (Y), and 15 lanthanides from lanthanum (La, 57) to lutetium (Lu, 71) [1] that play a significant role in the development of civilization and human life [2]. There are approximately 200 rare earth minerals. However, only a limited number of minerals, e.g., bastnaesite, monazite, xenotime, and REE-bearing clay, have been exploited for the economic extraction of rare earth elements [3]. These elements are critical for the production of high-tech products, devices, and technologies with extensive applications in the medical, defense, aerospace, and automobile industries [4]. Driven primarily by the anticipated exponential increase in electric vehicle and windmill production, the demand for REE minerals will grow and eventually exceed supply, which has recently fueled exploration activities and the development of mine and processing complexes to recover rare earth-containing minerals [5]. Alternatively, many major REE-consuming countries, including the United States, are evaluating non-conventional resources, including coal-based sources, mine waste, and acid mine drainage for the extraction of rare earth elements to meet demand ([6]–[8]).

Chi et al. described the use of either solvent extraction [9] and/or precipitation [2] for the recovery of the dissolved REEs from a pregnant leach solution. The upgrading of REEs by precipitation is possible due to the higher solubility of the cationic impurities, e.g., aluminum, iron, and zinc, as compared to rare earth carbonates and oxalates [10]. Strauss regarded oxalic acid ($H_2C_2O_4$) and sodium/ammonium carbonate ($Na_2CO_3/(NH_4)_2CO_3$) as the primary precipitating agents for the recovery of REEs. It was found that soda ash requires higher pH values for effective precipitation and does not offer optimum selectivity at higher concentrations of impurities including zinc, aluminum, and iron in the solution [11].

Alternatively, oxalic acid provides higher selectivity at lower pH values in the presence of high levels of impurities ([12], [11]). The selectivity of REEs towards oxalic acid is reported to be due to the strong affinity of REE^{3+} to the oxalate anions and extremely low solubility of rare earth oxalates ([13], [14]). The oxalate anion ($C_2O_4^{2-}$) is the conjugate base of oxalic acid, and its structure is shown in Figure 1.

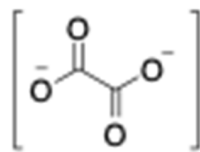
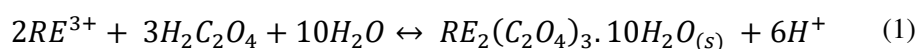


Figure 1. Structure of oxalate anions

Kim et al. also regarded REE crystallization using oxalic precipitation as the most significant REE preparation technology ([15], [16]). As such, it is frequently utilized in the industry due to its simplicity and high efficacy [17]. Oxalic acid precipitation is described by the following reaction mechanism:



66 Eq. (1) shows the production of six H⁺ ions for every three oxalate molecules added. According
67 to Le Chatelier's Principle, the reaction also explains the reason for a decline in precipitation
68 efficiency with a decrease in the solution pH value.

69 Chi et al. found that non-metallic cations such as Al³⁺, Fe³⁺, Mg²⁺, and Ca²⁺ present in the
70 pregnant leach solution either form complexes or precipitate with oxalic acid resulting in the
71 consumption of additional acid. This results in the need for a greater quantity of oxalic acid to
72 precipitate the REEs while also reducing precipitation efficiency [18]. Moreover, Woyski et al.
73 reported that excessive concentrations of iron also tend to impede the precipitation of REEs [19].

74 Kim et al. considered the acidity of the solution, oxalic acid concentration, and temperature
75 as the crucial experimental parameters required to optimize oxalic acid efficiency [15]. M.L Straus
76 reported that the pH of the solution is inversely proportional to oxalate solubility [11]. Chi et al.
77 found that REE recovery increases with an increase in pH[18]. However, the purity of the
78 precipitates decreases owing to the precipitation of impurities such as Al(OH)₃ and Fe(OH)₃. The
79 increased recovery with pH is in accordance with Le Châtelier's principle, which states that
80 increasing the pH shifts the equilibrium to the left [14]. Xia et al. reported in their patent that oxalic
81 acid precipitation at elevated temperatures of 75-100°C produces strong and fully formed crystals
82 that are easier to filter [20]. However, REE recovery seems to decrease with an increase in
83 temperature. Contrarily, M.L Strauss found the effect of temperature on REE recovery to be
84 inconclusive [11].

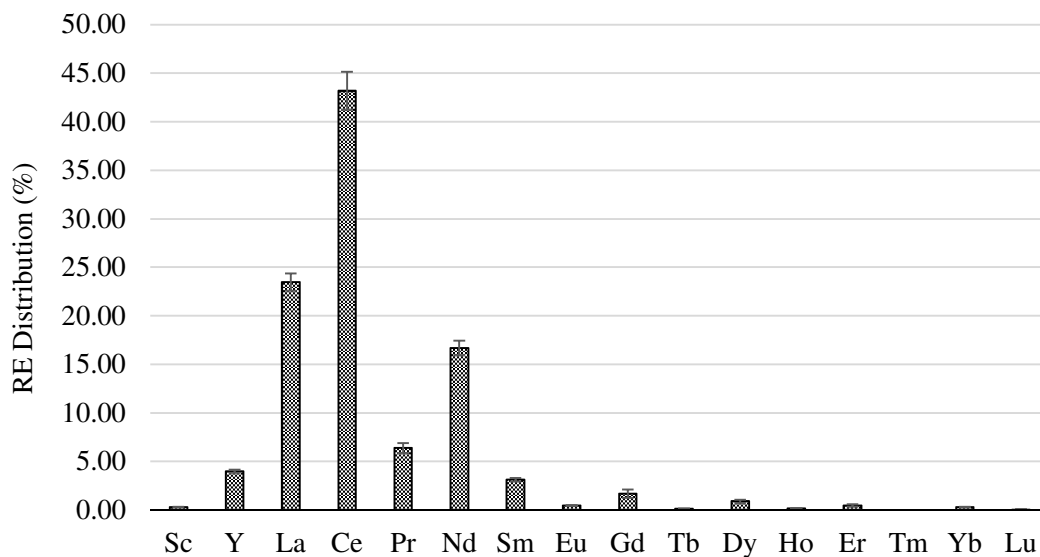
85 In this study, a parametric investigation was performed to analyze the impact of oxalic acid
86 dosage, precipitation pH, temperature, and the ferric ion concentration on RE-oxalate precipitation
87 efficiency. The tests were conducted over a wide temperature range while adjusting and
88 maintaining the solution pH at different levels by the addition of pH modifiers. The findings are
89 believed to be applicable to pregnant leach solutions containing contaminant ions at concentrations
90 equal to or greater than the total REE content.

91 **2. Materials and Methods:**

92 **2.1 Materials:**

93 The REE feedstock solution used in this study was generated from West Kentucky No. 13
94 coal seam coarse refuse material discarded from a coal preparation plant. The coarse refuse
95 material was processed through physical beneficiation and hydrometallurgical circuit in a pilot-
96 scale plant affiliated with the University of Kentucky located in Webster County, Kentucky. The
97 material was air-dried and processed through an X-Ray sorter where the REE content in the solid
98 was upgraded by isolating the lower density fractions. Next, the upgraded solid material was
99 crushed and ground through a jaw crusher and hammer mill, respectively, to produce a top size of
100 1 mm particle. The hammer mill product was roasted in a continuously operated tube furnace with
101 an inner tube temperature of 600 °C and a residence time of 20 minutes. The roasted material was
102 then leached using 0.05 M sulfuric acid at 75°C with a solid concentration of 100 g/L. The pH
103 value of the pregnant leachate solution (PLS) was 3.19±0.11 and contained about 9.5 ppm of total
104 REEs (TREEs), 93 ppm of Al, and 800 ppm of Fe. The PLS was further upgraded using multiple
105 stages of precipitation and redissolution. About 45% of the aluminum was removed by elevating

106 the pH to 4.3 using 2M NaOH. Subsequently, the REEs were precipitated at pH 7.0 using 2M
 107 NaOH. The precipitated REE sludge, which contained Al and Fe, was then re-leached using an
 108 HCl solution having a pH of 2.5 to selectively dissolve REEs in a concentrated solution. The re-
 109 leached PLS contained 34.6 ± 1.52 ppm of TREE with a distribution shown in Figure 2. The
 110 solution concentration of the primary contaminant ions was 60.8 ± 2.35 ppm, Al, 129.1 ± 10.54 ppm
 111 Ca, and 149.3 ± 7.19 ppm Fe. This solution served as the feedstock for the oxalic acid precipitation
 112 experiments conducted in this study.



113
 114 Figure 2. Rare-earth element distribution in the feedstock solution sums up to 100%

115 **2.2 Methods:**

116 *2.2.1- Experimental Procedure*

117 A 1% (w/v) Fe stock solution was prepared using iron(III) chloride hexahydrate
 118 ($\text{FeCl}_3 \cdot 6\text{H}_2\text{O}$, analytical grade >99% pure) purchased from Fisher Scientific. Each test started
 119 with adding the designated amount of 1% Fe^{3+} solution into 100 ml of REE pregnant feedstock
 120 solution in a 250 ml round-bottom flask manufactured by Pyrex. The solution was agitated on a
 121 magnetic stirring plate with a mixing speed of 400 rpm (estimate from the dial) and pre-heated to
 122 the required temperature in a temperature-controlled water bath. The oxalic acid solution prepared
 123 at various concentrations was added to the solution at a dosage of 4 ml per 100 ml after the desired
 124 temperature was achieved. The pH of the solution was modified as per the test requirement using
 125 4M NaOH or trace metal grade HCl and monitored with a Thermo Scientific Orion-Versastar pro
 126 meter after each adjustment. The reaction time started after the pH of the system stabilized at the
 127 desired setpoint. Subsequently, the samples were collected at time periods of 5, 10, 20, 30, and 60
 128 minutes. The collected samples were filtered directly after collection to stop the reaction using a
 129 33-mm syringe filter by Fisherbrand having a $0.45 \mu\text{m}$ pore size. A 1-ml sample was collected from
 130 the filtrate and diluted in 9 ml of 5% (v/v) trace metal grade HNO_3 . The chemical reagents utilized
 131 in this study were ACS grade or higher. The glassware was cleaned and rinsed properly with
 132 deionized water after each test and before re-use in subsequent tests.

133 2.2.2- *Operating Parameters:*

134 The process parameters evaluated in this study were oxalic acid concentration, pH,
135 temperature, and Fe (III) contamination in the solution. The oxalic acid solutions for the tests were
136 prepared at concentrations of 40, 80, 120, and 160 g/L, which were selected on the basis of the
137 stoichiometric ratios of the REE and contaminant ion concentrations in the feed leach solution.
138 The oxalic acid solution was prepared in deionized (DI) water and dissolved completely with an
139 ultrasonic bath. Each test used a fixed 4ml of the oxalic acid solution per 100 ml PLS throughout
140 the experimental plan. The range of solution pH values was 0.5 to 2.5 based on the oxalate species
141 distribution and its effectiveness above and below the stated range. The lowest temperature
142 covered in this study was 12.5 °C, which was maintained by constantly adding cold water into the
143 water bath, whereas the highest temperature was 62.5 °C. A 1% Fe solution was prepared for the
144 test plan and then added in the range of 0-400 ppm (representing 0-4 ml Fe(III)) according to each
145 test requirement. The stock solution used in this study had an initial 150 ppm concentration of Fe
146 present in the solution. The Fe contamination was based on the extra Fe added. Therefore, the total
147 Fe content was the sum of the initial concentration (150 ppm) and the concentration added. Each
148 test was run for a total of one hour, with samples extracted after 5, 10, 20, 30, and 60 minutes from
149 test initiation.

150 2.2.3- *Parametric Test Design*

151 A central composite design (CCD) was established using the Design-Expert software with
152 oxalic acid dosage, pH, temperature, and iron content of the solution as the four factors selected to
153 study. Five levels of variables were considered for each factor with an alpha value of 1.5, which
154 shows the distance of each axial point from the center in CCD. The test parameters and their
155 respective parameter levels used for the experiment design obtained from a Design Expert software
156 package are shown in Table 1.

157 Table 1. Operational parameters and their corresponding levels studied using a central composite design
158 to assess their impact on the efficacy of the oxalic acid precipitation process.

Factors	name	unit	Coded variable level				
			lower	low	center	high	higher
A	Oxalic Acid Solution Concentration	g/L	0	40	80	120	160
B	Temperature	°C	12.5	25	37.5	50	62.5
C	Fe Stock Solution Addition	ppm	0	100	200	300	400
D	pH	-	0.5	1	1.5	2	2.5

159

160 2.2.4- *Analysis (ICP)*

161 The feed and filtrate samples collected from each test were analyzed using a Spectro Arcos
162 II Inductively Coupled Plasma-Optical Emission Spectrophotometer (ICP-OES). The ICP-OES
163 unit was operated in a 5% (v/v) nitric acid matrix. Calibration was performed using a multi-element
164 certified reference standard of the following concentrations: 0 µg/mL, 0.05 µg/mL, 0.5 µg/mL, 1
165 µg/mL, 5 µg/mL, and 10 µg/mL. The calibration standard was the VHG SM68 Standard 1
166 purchased from the LGC Standards. Quality control was performed by two independently-sourced
167 check standards at a frequency of not less than every 20 samples. The recovery of these check

standards was within +/- 10% RSD. Due to the low concentration of REEs in solution, the lower limit of quantification of the ICP was examined by analyzing a series of sample with known concentration and the lower quantifiable limit is 0.001 ppm for Sc, Y, Nd, Eu, Yb, and Lu, 0.005 ppm for Sm and Dy, 0.05 ppm for Er, Pr, Tb, Ho, and Tm, 0.1 ppm for La, and 0.25 ppm for Ce and Gd. The REE precipitation efficiency values were calculated using the following expression:

$$\% PE = \frac{C_f * V_f - C_l * V_l}{C_f * V_f} * 100 \quad (\text{Eq. 1})$$

where PE is the precipitation efficiency, and C_f and C_l the total REE content in the feed and the filtered liquid sample after precipitation, respectively. V_f and V_l are the volumes of the feed and liquid samples, respectively. The volume of the filtered liquid included the total volume of chemical reagents added in each test.

3. Results and Discussion:

3.1 Experimental Results

The central composite design required 30 experiments to optimize REE precipitation efficiency. The individual test conditions and the corresponding response variable values are shown in Table 2. The experimental plan also included five duplicate tests to establish the repeatability of the study. The repeat tests in Table 2 are Run 6, 7, 11, 25, 26, and 29. The results indicated that the replicated tests have a 95% confidence interval of 0.575 for REE precipitation efficiency, which indicates excellent repeatability. The standard deviation of the REE precipitation efficiency of the five repeat tests was less than 1%. The highest REE precipitation efficiency of 99.88% was achieved at 120 g/L oxalic acid concentration, 25°C with 100 ppm Fe (III) contamination at pH of 2. However, the lowest precipitation efficiency value was 0% in tests 4 and 8, as shown in Table 2.

Table 2. The set of parametric values and corresponding REE precipitation efficiency value for each of the tests performed as part of the central composite design.

Run	Oxalic Acid Concentration (g/L)	Temperature (°C)	Fe Addition (ppm)	pH	REE Precipitation Efficiency (%)
1	40	50	100	1	0.83
2	80	12.5	200	1.5	99.1
3	40	50	100	2	69.0
4	80	37.5	200	0.5	0.00
5	40	25	100	1	50.0
6	80	37.5	200	1.5	94.5
7	80	37.5	200	1.5	94.5
8	40	50	300	2	0.00
9	0	37.5	200	1.5	4.3
10	120	25	300	1	91.6

11	80	37.5	200	1.5	94.0
12	120	25	100	1	95.0
13	40	25	300	2	0.63
14	80	37.5	0	1.5	94.3
15	120	25	100	2	99.9
16	40	50	300	1	5.4
17	120	50	100	1	68.8
18	80	37.5	400	1.5	79.1
19	120	50	300	2	96.6
20	40	25	300	1	0.82
21	120	50	300	1	68.2
22	120	25	300	2	97.4
23	80	62.5	200	1.5	79.7
24	120	50	100	2	97.5
25	80	37.5	200	1.5	95.4
26	80	37.5	200	1.5	95.3
27	160	37.5	200	1.5	94.6
28	40	25	100	2	95.5
29	80	37.5	200	1.5	95.1
30	80	37.5	200	2.5	98.9

192

193 3.2 Effect of major variables

194 3.2.1- Effect of Oxalic Acid Concentration:

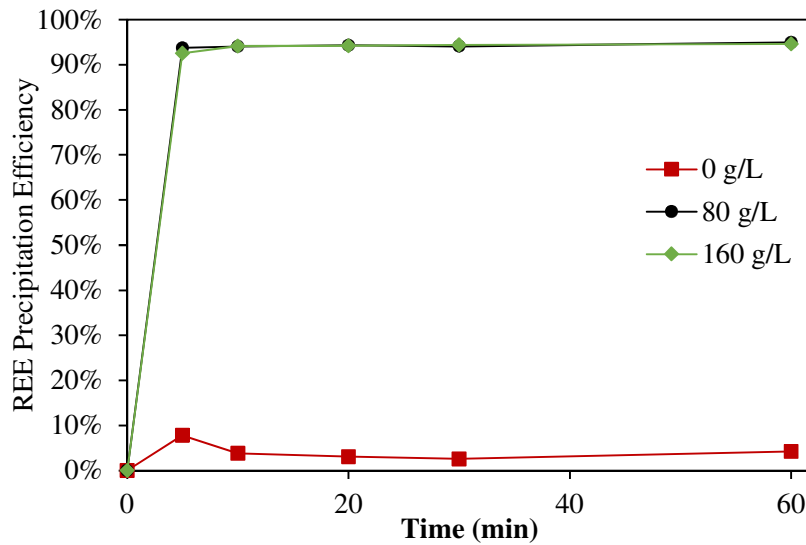
195 The oxalic acid dosage has a direct effect on the REE precipitation efficiency. This
196 association can be attributed to the fact that the higher oxalic acid concentration results in elevated
197 oxalate anion content in the solution. The major reactions that consume oxalate ions in solution
198 are the formation of RE-oxalate precipitates and the formation of iron and aluminum oxalate
199 complexes, as shown in Table 3. The equilibrium constants of these reactions were either adapted
200 from literature or calculated from the solubility product constant from literature. It is evident from
201 Table 3 that the precipitation of RE oxalates are the dominant reactions in the solution as the
202 equilibrium constant K for the RE-oxalate formations is significantly higher than that of the Fe
203 and Al oxalate complexes formation. However, the concentration of Fe³⁺ and Al³⁺ are orders of
204 magnitude higher than the REEs in the solution. As a result, the amount of oxalate ions occupied
205 by Fe³⁺ and Al³⁺ in the solution is still substantial. Other than Fe³⁺ and Al³⁺, a small quantity of
206 oxalate ions is occupied by Fe²⁺ and Ca²⁺ to form calcium oxalate and ferrous oxalate. An optimal
207 dosage of oxalic acid exists where the oxalate ions satisfy the needs for RE-oxalate precipitation
208 and form soluble iron and aluminum oxalate complexes, yet minimum amount of calcium and

209 ferrous oxalate. Decreasing the oxalic acid dosage is detrimental to the RE-oxalate precipitation
 210 efficiency, whereas increasing the oxalic acid dosage promotes the formation of impurities.

211 The test data allows a direct comparison of oxalic acid concentration effects at values of 0,
 212 80, and 160 g/L while maintaining the values of the other process parameters at constant values.
 213 As shown in Figure 3, it was observed that there is a significant variation in the recovery of rare
 214 earth elements when the dosed reagent concentration is increased from 0-80 g/L. Interestingly, it
 215 was observed that a minor concentration of REEs precipitated even without the addition of oxalic
 216 acid. According to Han (2019), RE³⁺ ions tend to form complexes with anions such as Cl⁻, NO₃⁻,
 217 and SO₄²⁻ at lower pH levels and subsequently precipitate ([20],[21]). Increasing the oxalic acid
 218 concentration from 80-160 g/L did not improve REE precipitation efficiency. This trend is in
 219 agreement with the findings reported by other researchers ([22],[26],[28]). Consequently, the
 220 addition of surplus oxalic acid, i.e., 160 g/L, increased the Fe-contamination of rare earth
 221 precipitates by as much as 5% as compared to lower dosages of the reagent discussed above. A
 222 possible reason behind this might be that the excessive oxalate ion in solution promoted the
 223 reduction of Fe (III) to Fe (II), then formed ferrous oxalate as a precipitate. The reaction details
 224 and fundamentals are discussed later in the paper.

225 Table 3. The equilibrium constants of RE-oxalate precipitation and other metal oxalate complexes
 226 formation reactions (adapted from [24]–[27]).

Reaction	LgK	Reaction	LgK
$2\text{Ce}^{3+} + 3\text{C}_2\text{O}_4^{2-} \rightleftharpoons \text{Ce}_2(\text{C}_2\text{O}_4)_3 (\text{s})$	30.18	$\text{Al}^{3+} + 3\text{C}_2\text{O}_4^{2-} \rightleftharpoons \text{Al}(\text{C}_2\text{O}_4)_3^{3-}$	17.09
$2\text{Y}^{3+} + 3\text{C}_2\text{O}_4^{2-} \rightleftharpoons \text{Y}_2(\text{C}_2\text{O}_4)_3 (\text{s})$	28.27	$\text{Al}^{3+} + 2\text{C}_2\text{O}_4^{2-} \rightleftharpoons \text{Al}(\text{C}_2\text{O}_4)_2^-$	13.41
$2\text{Nd}^{3+} + 3\text{C}_2\text{O}_4^{2-} \rightleftharpoons \text{Nd}_2(\text{C}_2\text{O}_4)_3 (\text{s})$	31.11	$\text{Al}^{3+} + \text{C}_2\text{O}_4^{2-} \rightleftharpoons \text{Al}(\text{C}_2\text{O}_4)^+$	7.73
$2\text{La}^{3+} + 3\text{C}_2\text{O}_4^{2-} \rightleftharpoons \text{La}_2(\text{C}_2\text{O}_4)_3 (\text{s})$	28.22	$\text{Fe}^{3+} + 3\text{C}_2\text{O}_4^{2-} \rightleftharpoons \text{Fe}(\text{C}_2\text{O}_4)_3^{3-}$	19.83
$2\text{Sm}^{3+} + 3\text{C}_2\text{O}_4^{2-} \rightleftharpoons \text{Sm}_2(\text{C}_2\text{O}_4)_3 (\text{s})$	31.35	$\text{Fe}^{3+} + 2\text{C}_2\text{O}_4^{2-} \rightleftharpoons \text{Fe}(\text{C}_2\text{O}_4)_2^-$	15.45
$2\text{Eu}^{3+} + 3\text{C}_2\text{O}_4^{2-} \rightleftharpoons \text{Eu}_2(\text{C}_2\text{O}_4)_3 (\text{s})$	31.38	$\text{Fe}^{3+} + \text{C}_2\text{O}_4^{2-} \rightleftharpoons \text{Fe}(\text{C}_2\text{O}_4)^+$	9.15
$2\text{Gd}^{3+} + 3\text{C}_2\text{O}_4^{2-} \rightleftharpoons \text{Gd}_2(\text{C}_2\text{O}_4)_3 (\text{s})$	31.37	$\text{Fe}^{2+} + 2\text{C}_2\text{O}_4^{2-} \rightleftharpoons \text{Fe}(\text{C}_2\text{O}_4)_2^{2-}$	5.9
$2\text{Dy}^{3+} + 3\text{C}_2\text{O}_4^{2-} \rightleftharpoons \text{Dy}_2(\text{C}_2\text{O}_4)_3 (\text{s})$	30.70	$\text{Fe}^{2+} + \text{C}_2\text{O}_4^{2-} \rightleftharpoons \text{FeC}_2\text{O}_4(\text{aq})$	3.97
$2\text{Er}^{3+} + 3\text{C}_2\text{O}_4^{2-} \rightleftharpoons \text{Er}_2(\text{C}_2\text{O}_4)_3 (\text{s})$	30.05	$\text{Ca}^{2+} + \text{C}_2\text{O}_4^{2-} \rightleftharpoons \text{CaC}_2\text{O}_4(\text{aq})$	3.19
$\text{Ca}^{2+} + \text{C}_2\text{O}_4^{2-} \rightleftharpoons \text{CaC}_2\text{O}_4 (\text{s})$	8.65	$\text{Fe}^{2+} + \text{C}_2\text{O}_4^{2-} \rightleftharpoons \text{FeC}_2\text{O}_4 (\text{s})$	6.69



228

229
230

Figure 3 Comparison of REE precipitation efficiency at various concentrations of oxalic acid and fixed pH=1.5, temp=37.5°C, and 200 ppm Fe addition

231 *3.2.2- Effect of pH*

232

233

234

235

236

237

238

239

240

241

242

This investigation revealed a positive correlation between solution pH and REE precipitation efficiency. Highly acidic conditions did not produce any rare earth precipitates, likely due to the concentration of H⁺ ions which suppresses the reaction between the REEs and the oxalate according to Eq. (1). As shown in Figure 5, the reduction in H⁺ concentration resulting in a rise in the solution pH to 1.5 dramatically improved REE precipitation efficiency to 94.8%, and a further increase to pH 2.5 elevated the efficiency to 98.9%. It is also worth mentioning that higher pH levels reduce the oxalic acid dosage required for REE-precipitation due to the increased oxalate anions concentration present in the less acidic solution. This observation agrees with the findings reported by Zhang et. al. which showing that an elevated pH value promoted the dissociation of oxalic acid molecules which improved RE precipitation efficiency at lower oxalate dosages [24]. The solution chemistry is discussed in detail later in this publication.

243

244

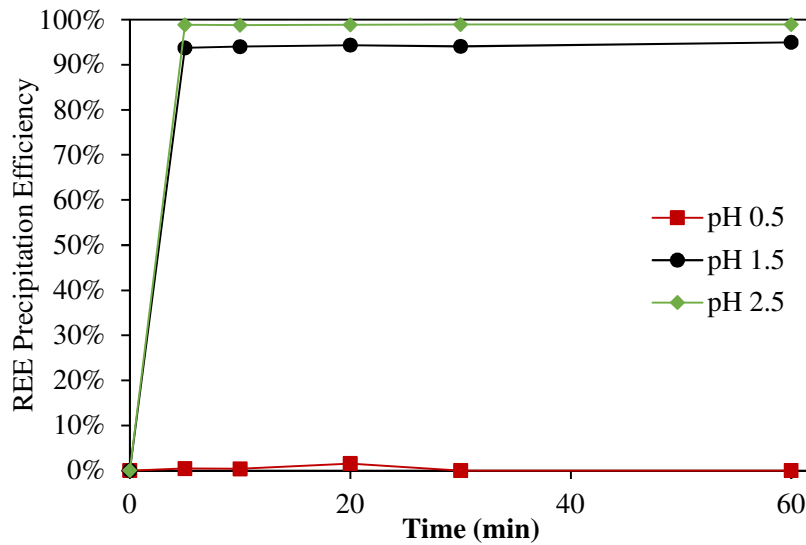
245

246

247

248

The investigation also revealed a decrease in the REE precipitate purity with an increase in pH. The Fe and Al recovery increased by as much as 8% and 5%, respectively, while raising the pH from 1.5 to 2.5, reaffirming previously reported findings ([18], [28], [29]). Based on these results, a pH value within the range of 1.0 – 2.0 maximizes REE recovery and product purity. Considering that lower solution pH values generally require higher oxalic acid dosages as well as the cost of acid to modify the pH, a pH between 1.5-2.0 is likely more economically desirable.

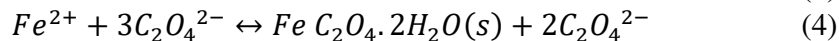
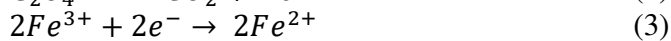


249

250 Figure 4 Effect of pH on the REE precipitation efficiency at 80g/L oxalic acid concentration, 200 ppm Fe
 251 addition, and 37.5°C temperature

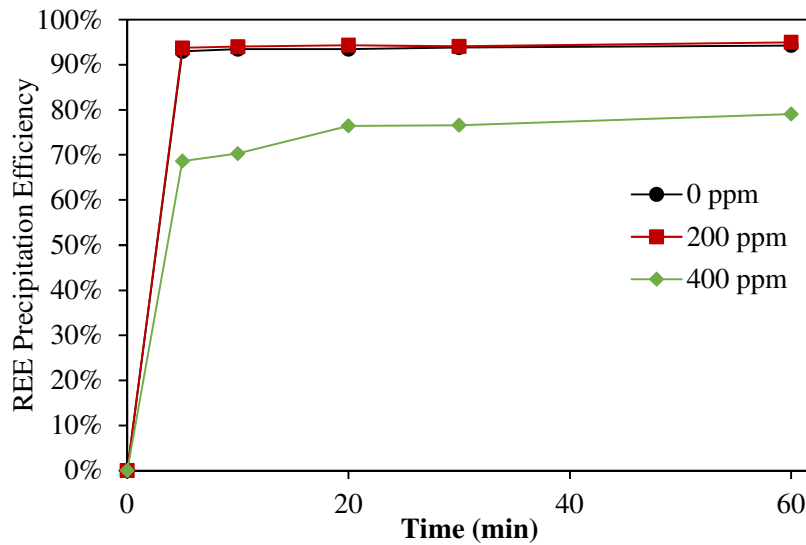
252 3.2.3- *Effect of iron contamination:*

253 Several researchers have reported the Fe reduction properties of oxalate anions [30]–[32].
 254 The oxalate anions have two oxygen atoms with unshared pairs of electrons, making the ion a
 255 strong complexing agent. In the presence of ferric and aluminum ions, the oxalate ions tend to
 256 form chelate complexes with these impurities, thereby resulting in a soluble complex ([33],[34]).
 257 Ferric oxalates [Fe₂(C₂O₄)₃] have high stability in oxalic acid solution. However, ferrous oxalates
 258 (FeC₂O₄·6H₂O) are highly insoluble ([35], [36]). Therefore, it can be concluded that Fe-
 259 contamination of RE-oxalates in an oxalate system is possible by the reduction of Fe(III) to Fe(II).
 260 The reduction of oxalate and, consequently, Fe is possible through reactions below:



261

262 As ferric ion is one of the dominant contaminant ions obtained from the upstream process
 263 in REE-bearing leachate solution in this investigation, the additional Fe(III) contamination dosed
 264 was changed from 0 to 400 ppm in the stock solution to examine the influence of Fe on the REE
 265 precipitation efficiency. It is shown in Figure 5 that the addition of iron up to 200 ppm does not
 266 significantly impact the REE precipitation efficiency. A further increase in the Fe-contamination
 267 to 400 ppm significantly drops the REE precipitation efficiency from 94.8% to 79.1%. The
 268 findings of this study agree with Woyski et al., who also reported that excessive concentrations of
 269 iron also tend to impede the precipitation of REEs [19]. As per Christodoulou et al. [30], the
 270 formation of ferric oxalates as chelate complexes consumes oxalate anions, thereby decreasing the
 271 oxalate anion content available for RE-oxalate formation, which, in turn, reduces the REE
 272 precipitation efficiency. According to Venkatesan et al. ([37],[38]), this problem can be addressed
 273 by increasing the oxalic acid dosage in the system.

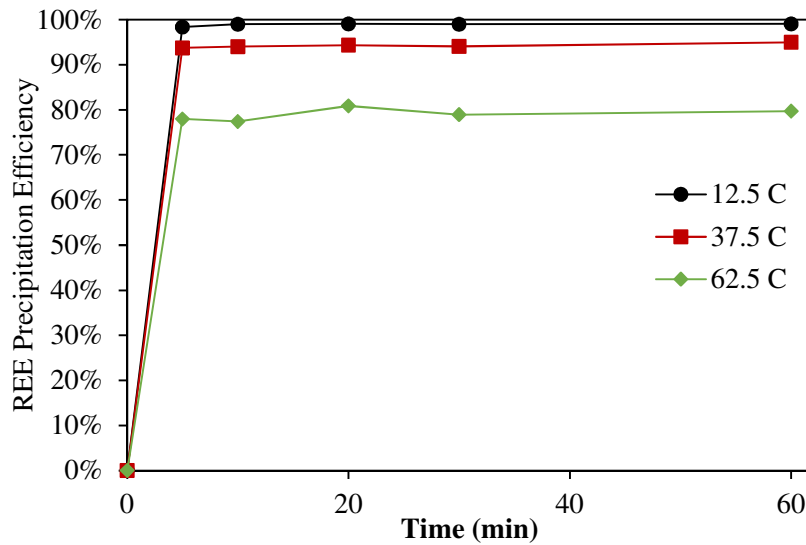


274

275 Figure 5 Impact of different Fe(III) contamination levels on the REE precipitation efficiency at 80g/L
 276 oxalic acid concentration, pH 1.5 and 37.5°C

277 *3.2.4- Effect of temperature:*

278 The dependence of REE precipitation efficiency on temperature was ascertained by
 279 performing experiments at 12.5, 37.5, and 62.5 °C. It was determined that there is an inverse
 280 association between the temperature and precipitation of rare earth elements, as shown in Figure
 281 6, which is indicative of an exothermic reaction. The REE precipitation efficiency increases with
 282 a decrease in temperature with a maximum recovery of 99.1% obtained at 12.5 °C. The solubility
 283 of rare earth elements and oxalic acid has been reported to increase with an increase in temperature,
 284 owing to the dissociation of oxalic acid ([39],[40]). Furthermore, according to Le Chlatelier's
 285 principle, increasing the reaction temperature shifts the reaction in the reverse direction.
 286 Consequently, the REE precipitation efficiency decreases from 99.1% to 94.8% at 37.5 °C, and
 287 ultimately to its lowest point of 79.7% at 62.5 °C.



288

289 Figure 6 Effect of temperature on the REE precipitation efficiency with 80g/L oxalic acid concentration at
 290 a dosage of 160 ml/L PLS, pH 1.5, and additional 200ppm iron contamination

291 **3.3 Quadratic Regression Model**

292 The results of the central composite factorial experimental design performed for the estimation
 293 of rare earth precipitation efficiency are given in Table 2. The reduced quadratic regression model
 294 expression for the response was obtained from Design-Expert software, and the semi-empirical
 295 model after the elimination of insignificant coefficients can be expressed as follows:

296
$$\text{ArcSin}(\text{Sqrt}(\text{REE precipitation efficiency})) = 1.25 + 0.3728 * A - 0.1068 * B - 0.1461 * C + 0.2214 * D + 0.161 * AC - 0.1529 * A^2 - 0.1628 * D^2$$

 297 (Eq. 2)

298 where A is the oxalic acid solution concentration (g/L), B is the temperature (°C), C is the iron
 299 contamination (x100 ppm), and D is the solution pH. The significance of the model, individual
 300 parameters, and their interactions was tested against the null hypothesis that the coefficient for the
 301 variable is null. The parameters with a p-value < 0.05 were deemed significant. The forward
 302 elimination method was used to remove all insignificant parameters, and the model efficacy was
 303 determined through a higher adjusted R² value of the best fit model. Furthermore, the investigation
 304 of residual errors for the selected model revealed an independent distribution of errors with
 305 constant variance and zero mean.

306 The acquired quadratic regression model and its significance are shown in Table 4. The p-
 307 value <0.05 indicates that the overall model is highly significant for predicting REE precipitation
 308 efficiency. The R² and adjusted R² values of 84.89% and 80.08%, respectively, also suggests a
 309 good fit for the model. Additionally, as demonstrated in Table 5, all the parameters used in this
 310 investigation were found to impact the REE recovery substantially. Figure 8 shows the impact of
 311 individual parameters on REE precipitation efficiency as predicted by the model.

312 Oxalic acid dosage and solution pH clearly have the greatest effect on REE precipitation,
 313 which is directly tied to the impact on the chemical reaction between the oxalate anions and the

314 REEs (Eq. 1). The oxalic acid dosage and pH showed strong positive correlations, whereas solution
 315 temperature and Fe content had a negative impact on REE precipitation efficiency. The
 316 investigation also revealed an interaction between the oxalic acid dosage and the iron content of
 317 the solution, which was previously described to be a result of iron reduction and complexation
 318 with the oxalate anion. This interaction effect estimated at 37.5°C and pH 1.5 is shown in Figure
 319 8 as a 3-D response surface. This 3-D response graph reiterates the points made earlier in the paper
 320 that higher oxalic acid concentrations are required for high Fe(III) contaminated feed solutions to
 321 achieve optimum REE precipitation efficiency. It is evident that, at concentrations above 100g/L,
 322 the response surface becomes smoother at all Fe contaminations. This implies that there are enough
 323 oxalate anions available in the solution to react with both REEs and Fe(III) cations. Furthermore,
 324 it can be concluded that oxalic acid dosage can be minimized by reducing the iron content in the
 325 pregnant leach solution feeding the process.

326 Table 4 The analysis of variance (ANOVA) table for the suggested REE precipitation efficiency model

Source	Sum of Squares	df	Mean Square	F-value	p-value
Model	6.99	7.00	0.9987	17.66	<0.0001
Residual	1.24	22.00	0.056		
Total	8.24	29.00			

327

328 Table 5 The ANOVA for the parameters of the suggested REE precipitation efficiency model

Source	Sum of Squares	df	Mean Square	F-value	p-value
A-Oxalic Dosage	3.34	1	3.34	58.98	< 0.0001
B-Temperature	0.2735	1	0.2735	4.84	0.0387
C-Fe Addition	0.5126	1	0.5126	9.06	0.0064
D-pH	1.18	1	1.18	20.80	0.0002
AC	0.4147	1	0.4147	7.33	0.0129
A ²	0.6649	1	0.6649	11.76	0.0024
D ²	0.7538	1	0.7538	13.33	0.0014

329

330

331

332

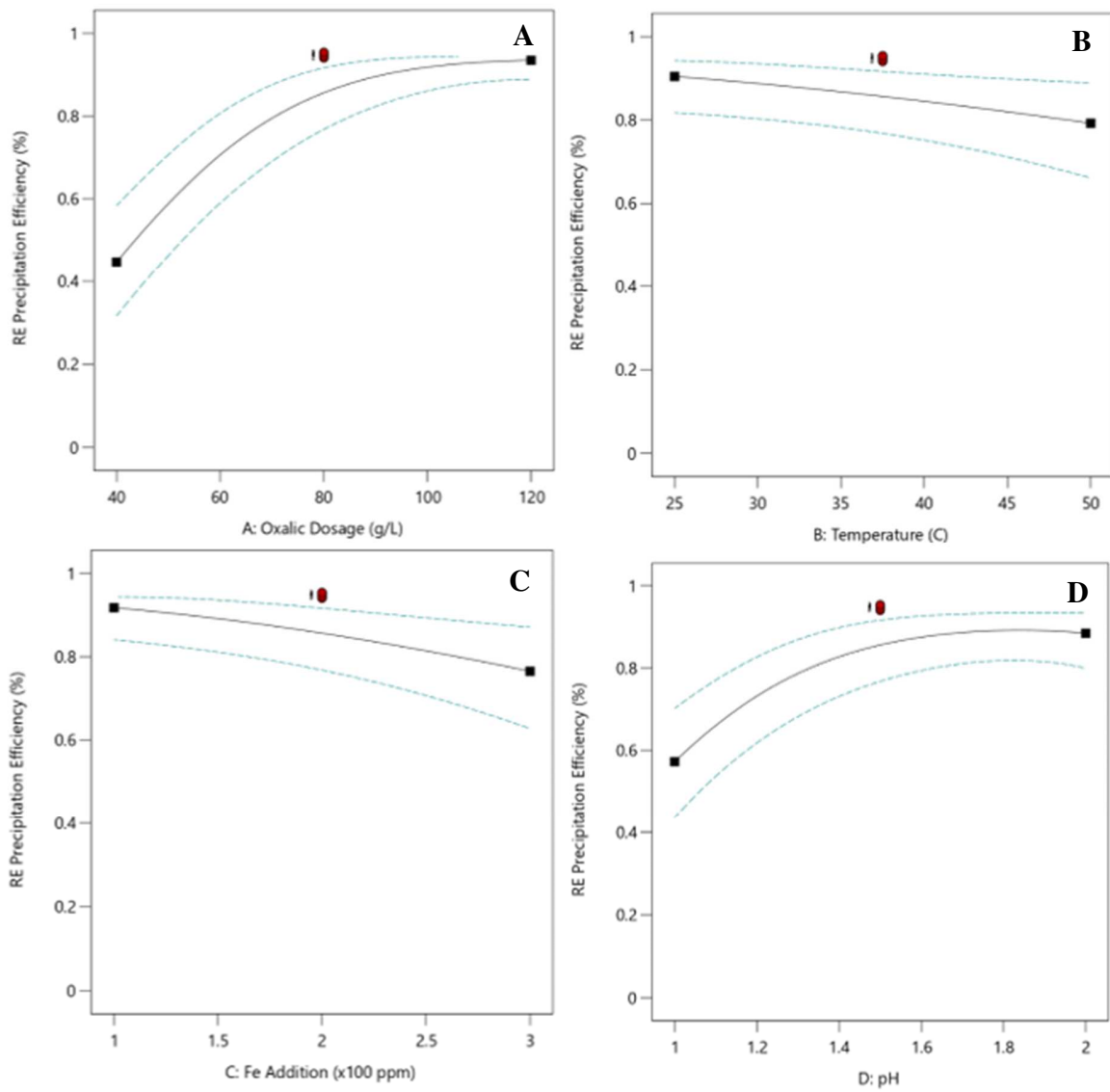
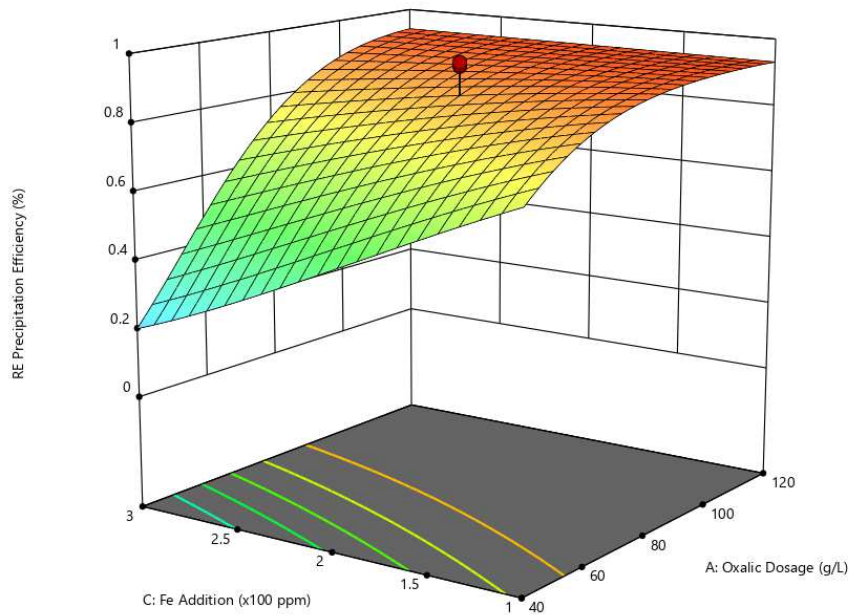


Figure 2 Impact of A: Oxalic acid dosage, B: Temperature, C: Fe Addition, and D: pH on REE precipitation efficiency (the dash lines represent the confidence interval).



334

335 Figure 8 Response surface showing the interactive effects of oxalic acid dosage and Fe addition on REE
 336 precipitation efficiency (Factor B: Temperature =37.5°C, Factor D: pH =1.5)

337 **3.4 Model Validation:**

338 The semi-empirical quadratic regression model was validated under the conditions which
 339 minimized the required oxalic acid dosage over a pH range of 1-2 range and various Fe
 340 contamination levels at a constant solution temperature of 25°C. The Fe content was selected based
 341 on a typical solution composition generated from REEs cake redissolution prior to REE oxalate
 342 precipitation. The pH range of 1-2 was selected based on the better purity of the rare earth
 343 precipitates formed between these two acidity levels. The validation test results, along with their
 344 conditions, are shown in Table 6. The predicted value for REE precipitation efficiency with Fe
 345 addition of 100 and 200 ppm were 83.9 and 76.4%, showing a good agreement with the actual test
 346 data, i.e., 82.4% and 79.8%, respectively.

347 Table 6. Comparison of predicted and actual oxalic acid precipitation efficiency data generated for a
 348 solution having a pH of 1.84 and temperature of 25°C.

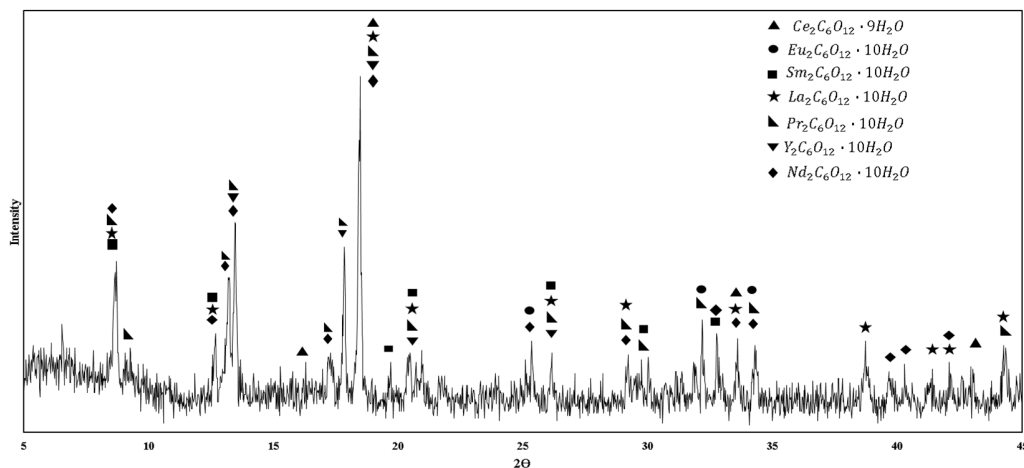
Number	Oxalic Dosage (g/L)	Temperature (°C)	Fe Addition (ppm)	pH	REE Precipitation Efficiency (%)	
					Predicted	Actual
1	35.71	25.00	100	1.84	83.9	82.4
2	49.64	25.00	200	1.84	76.4	79.8

349

350 **3.5 Production of rare earth oxalate**

351

352 The feedstock solution was processed in a pilot plant facility to generate a high grade mixed
 353 rare earth oxalate product. The circuit was comprised of three 55-liter cone bottom mixing tanks
 354 in sequence. The first tank was equipped with a pH probe and transmitter that controls a peristaltic
 355 pump to automatically adjust pH by dosing a 4M NaOH solution. The feedstock solution and
 356 oxalic acid solution was fed into the first tank at a controlled flowrate. The total residence time
 357 was 20 minutes with the third tank serving as feed tank to a pressure filter. The filtration rate was
 358 held at a constant value to maintain the level of the third oxalic precipitation tank. The filter cake
 359 was dried in the oven at 75 °C for 24 hours. The dried solid was analyzed using X-ray diffraction
 360 (XRD) to confirm the composition of the oxalate product as shown in Figure 9. Since the XRD
 361 peaks of some of the REE oxalates share the same position, the intensity of the peaks was mostly
 362 contributed by several REE oxalates overlapping. The mixed rare earth oxalate sample was then
 363 roasted in a muffle furnace at 750 °C for 2 hours to convert rare earth oxalate to rare earth oxide
 364 (REO). The REO was then fully digested using trace metal grade nitric and hydrochloric acid and
 365 the liquid was subjected to elemental analysis using ICP-OES and ICP-MS unit. The elemental
 366 composition was then converted to the form of rare earth oxide with the corresponding
 367 stoichiometric ratio of rare earth element to oxygen. The grade of 92.6% REO product is shown in
 368 Table 7 along with the element-by-element content.



369
 370 Figure 9. XRD analysis of REE oxalate precipitate produced from the feedstock solution generated from
 371 mine refuse material in a pilot scale operation.

372 Table 7. The grade of rare earth oxides produced from rare earth oxalate precipitation.

RE Oxides	Sc ₂ O ₃	Y ₂ O ₃	La ₂ O ₃	CeO ₂	Pr ₆ O ₁₁	Nd ₂ O ₃	Sm ₂ O ₃	Eu ₂ O ₃	Gd ₂ O ₃
Weight (%)	0.04	3.98	17.04	41.99	4.85	17.16	3.07	0.54	2.15
RE Oxides	Tb ₄ O ₇	Dy ₂ O ₃	Ho ₂ O ₃	Er ₂ O ₃	Tm ₂ O ₃	Yb ₂ O ₃	Lu ₂ O ₃	Total	
Weight (%)	0.21	0.88	0.14	0.32	0.04	0.19	0.03	92.63	

373

374

375 **3.6 Solution chemistry study**

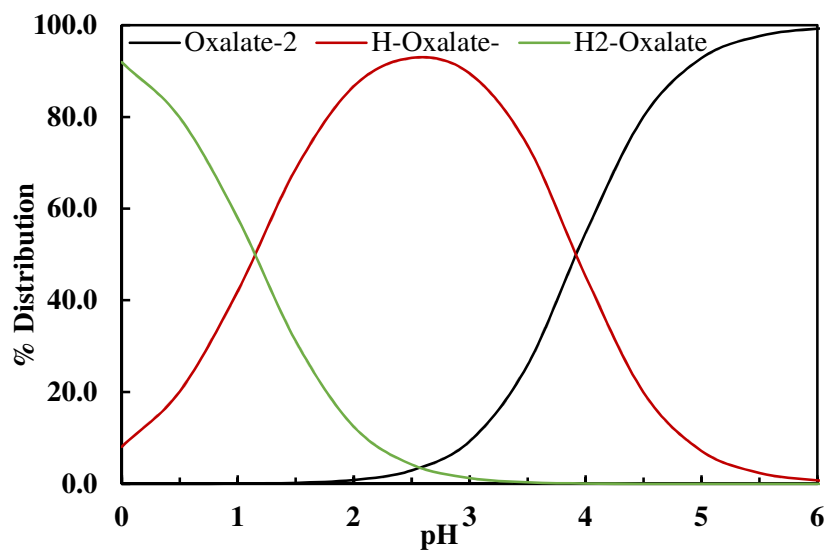
376 *3.6.1 Oxalate water system*

377 The reaction required for the REE precipitation begins by the dissociation of oxalic acid in
378 the solution, which can be expressed by the following reactions [41];



379 In the first step, the oxalic acid converts to hydrogen oxalate anion, which further
380 dissociates in the second step to produce the oxalate anions required for RE oxalate formation. As
381 per equations (5) and (6), the oxalate anion formation reaction releases two hydrogen ions, thereby
382 decreasing the solution pH.

383 The oxalic acid coexists with hydrogen oxalate and oxalate anions in equilibrium at any
384 given pH [34]. However, the dominant species present in the solution changes as a function of pH.
385 According to Figure 10, $H_2C_2O_4$ is a major species at $pH < 1$. As the pH rises above 1, hydrogen
386 oxalate becomes the significant species in the system. Furthermore, the model output indicated
387 that pH also influences the activity of oxalate anions, which are the primary precipitants for rare
388 earth precipitation, corroborating the findings of and Chi et. al. [18] and I. Bureau [23]. It is worth
389 mentioning that most of the REE reactions with oxalate anions are typically performed around pH
390 2. This is done to minimize the precipitation of contaminant metal ions as metal-oxalates. For pH
391 values, less than 2, the solution speciation shown in Figure 10 reveals oxalate anions have minimal
392 concentration and activity. Consequently, the oxalic acid dosage required for successful
393 precipitation increases significantly.

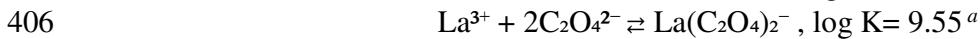
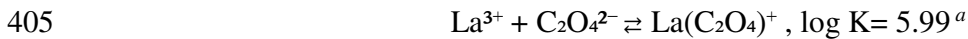
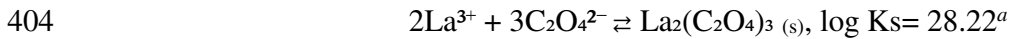


394
395 Figure 10. Species distribution of oxalic acid in water as a function of pH (oxalate concentration =0.1M,
396 25°C).

397 *3.6.2 RE-Oxalate precipitation*

398 To further understand the rare earth precipitation behavior in the oxalate system, studies
399 were performed to examine the speciation distribution in solution at equilibrium. Visual MINTEQ

400 3.1 software was utilized to conduct the equilibrium calculations. Since rare earth elements possess
401 similar chemical properties, lanthanum (La) was selected to perform the calculations for the La-
402 Oxalate precipitation system. The equilibrium reactions and the corresponding constants for La-
403 oxalate precipitation at 25 °C are expressed as:

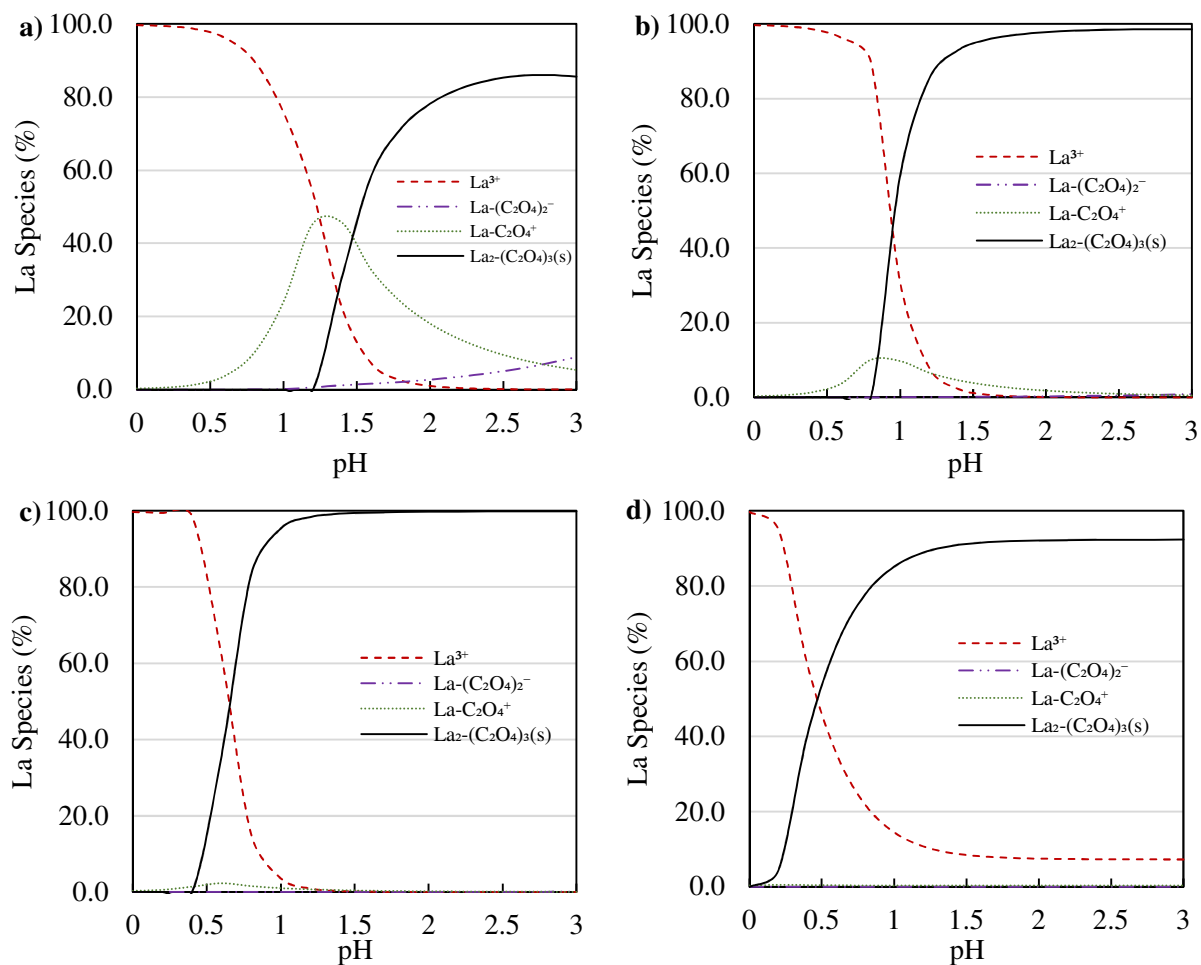


407 (^avalues obtained from Visual MINTEQ software).

408

409 The absolute concentration of rare earth elements significantly contributes to the
410 precipitation efficiency of RE-oxalate in solution at equilibrium. With 0.01M oxalate
411 concentration in the system, the stoichiometric concentration of La needed for the formation of
412 $\text{La}_2(\text{C}_2\text{O}_4)_3$ was calculated to be 1000 ppm ($\sim 7.2 \times 10^{-3}\text{M}$). Results in Figure 11 show that in a La-
413 oxalate system with 1000 ppm of La^{3+} and 0.01M of $\text{C}_2\text{O}_4^{2-}$, the precipitation of $\text{La}_2(\text{C}_2\text{O}_4)_3$ starts
414 to occur around pH 0.2 and the degree of reaction reaches >90% at pH >1.5. When the
415 concentration of La was reduced to 100 ppm, the excessive amount of oxalate ions prompted the
416 reaction to where >99% of La precipitated as pH 1.5. However, reducing the La concentration to
417 10 ppm, the precipitation curve shifted to a higher pH range due to the promoted formation of
418 $\text{La}(\text{C}_2\text{O}_4)^+$ under the excessive concentration of $\text{C}_2\text{O}_4^{2-}$. With one ppm of La, the peak precipitation
419 of 86% occurs at pH 2.8 and starts to show a downward trend with a pH increase due to the elevated
420 concentration of $\text{La}(\text{C}_2\text{O}_4)_2^-$.

421 Consequently, in the mixed rare earth leachate solution generated from mine waste
422 material, some of the rare earth elements with low concentration resulted in low precipitation
423 efficiency even with an excessive amount of oxalate. Comparing the four scenarios presented in
424 Figure 11, scenario c) is the optimal scenario where the precipitation completes at a lower pH,
425 thereby improving selectivity. However, scenarios a and b are more representative of a rare earth
426 leachate obtained from the treatment of typical mine waste and recycled materials where the REE
427 content is low relative to the leachable contaminant ions. The results indicate that increasing the
428 concentration of REEs in the oxalate precipitation feed solution would improve the oxalate
429 precipitation efficiency as well as selectivity due to the lower reaction pH.



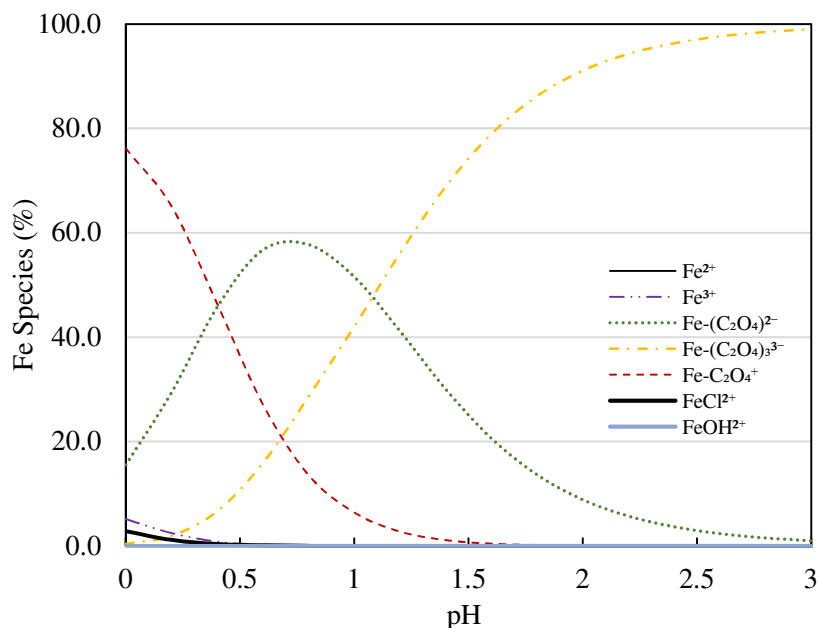
430

431

432 Figure 11. La species distribution in solution at equilibrium and La oxalate precipitation efficiency at a) 1
 433 ppm La^{3+} ; b) 10 ppm La^{3+} ; c) 100 ppm La^{3+} ; d) 1000 ppm La^{3+} with 0.01 M oxalate 25 °C simulated using
 434 Visual MINTEQ software. (The $\text{La}(\text{C}_2\text{O}_4)_3^{3-}$ and LaOH^{2+} species are calculated to be less than 0.1% in
 435 these four systems, therefore not included in the plots.)

436 3.6.3 Fe-Oxalate speciation

437 The concentration of Fe in both its ferric or ferrous forms directly influences the REE
 438 precipitation efficiency. The iron present in the solution can react with oxalate anions to form
 439 various species depending upon the pH of the system. Visual MINTEQ 3.1 software was used to
 440 simulate the speciation behavior of Fe at equilibrium. The developed speciation distribution shown
 441 in Figure 12 indicates that $\text{Fe}-(\text{C}_2\text{O}_4)_3^{3-}$, $\text{Fe}-(\text{C}_2\text{O}_4)_2^-$, and $\text{Fe}-(\text{C}_2\text{O}_4)^+$ are dominant species in the
 442 solution having a pH value between 0 and 3. The dominant species seems to change drastically
 443 with a relatively small change in the solution pH. Furthermore, there is only a minimal
 444 concentration of FeCl^{2+} , FeOH^{2+} , Fe^{2+} , and Fe^{3+} present in the same pH range. This phenomenon
 445 suggests that the ferric ion occupies the majority of the oxalate species in the solution generated
 446 from the mine waste material.



447

448 Figure 12. Fe species distribution in the precipitation system at equilibrium with 0.035M $C_2O_4^{2-}$, 0.1M
 449 Cl^- , 150 ppm Fe^{3+} , 60 ppm Al^{3+} , 130 ppm Ca^{2+} , and 35 ppm La^{3+} at 25 °C simulated using Visual
 450 MINTEQ software. (Species less than 0.01% were included in the calculation but not plotted)

451 It has been established in previous studies that iron oxalate precipitates in the ferrous form
 452 [30]–[32]. As oxalic acid is a mild reducing agent, an excessive addition of oxalic acid can reduce
 453 iron from ferric to ferrous thereby causing precipitation as ferrous oxalates by undergoing reactions
 454 (2)-(4) [42]. Therefore, it can be inferred that an excessive concentration of oxalic acid at lower
 455 concentrations of Fe(III) will reduce more iron to its ferrous form thereby decreasing the purity of
 456 rare earth precipitates. At high Fe(III) concentrations, a small portion will be reduced which will
 457 result in the precipitation of ferrous oxalate in a solid form while the remaining ferric iron will
 458 form various oxalate complexes and remain in solution.

459 In addition, the higher concentration of Fe(III) is also not desirable as it drastically reduces
 460 the REE precipitation efficiency. To thoroughly study its effect, various iron concentrations were
 461 analyzed using MINTEQ by varying the Fe^{3+} concentration between 150-950 ppm. The impact of
 462 the increase in Fe concentration with other species present in the system at typical concentrations
 463 is shown in Table 8. A significant increment in the concentration of iron-oxalate species in the
 464 solution was observed with an increase in Fe^{3+} concentration from 150-950 ppm. Furthermore, the
 465 free oxalate anion content drops from 0.149% to 0% when the Fe^{3+} concentration increases from
 466 150 to 950 ppm. It can be deduced that the additional iron in the system decreases the oxalate
 467 anions available for the reaction with REEs. As an example, Figure 13 predicts that lanthanum
 468 precipitation will significantly decline with a rise in iron concentration beyond 550 ppm. This
 469 finding is due to the lack of oxalate anions which is also shown in Table 8 by a content decrease
 470 from 0.039% at 550 ppm Fe to 0% at 950 ppm Fe. The maximum lanthanum precipitation of
 471 approximately 97% is predicted when the iron contamination is minimum, i.e., 150 ppm, which is
 472 the base concentration in the original PLS. It is noted that the impact of Fe concentrations between

473 150 ppm and 550 ppm on REE precipitation is insignificant, which indicates adequate availability
474 of oxalate anions. Correspondingly, the oxalate ions occupied by the RE ions as a precipitate is
475 approximately 1% of the total oxalate species when the ferric ion concentration is less than 550
476 ppm in solution. The oxalate ions consumed by REEs reduced significantly to 0.741% as ferric ion
477 concentration increased to 950 ppm which indicated the depletion of free oxalate ions due to ferric
478 ion complexation.

479 The findings from this simulation reaffirm the empirical findings from this study. The
480 experimental data also showed a decrease in the REE precipitation efficiency when the Fe(III)
481 contamination was increased from 100-400 ppm. The precipitation efficacy decreased from 94.8%
482 to 79.1% as a result of increasing the contamination from 100-400 ppm (corresponding to 1-4 ml).
483 It can be deduced that the decrease in efficacy is owing to the preferential reaction of oxalate
484 anions with Fe⁺³ cations instead of REEs present in the solution. It should be noted here that,
485 despite a preferential reaction taking place between the Fe⁺³ and oxalate anions, the ferric oxalate
486 anions do not precipitate, which results in a higher oxalic acid precipitation selectivity as compared
487 to other precipitating agents. Therefore, a high oxalic acid dosage is required in order to achieve
488 higher rare earth precipitation efficiency at higher iron contamination levels. The findings agree
489 well with those reported by Zhang et. al. (2020) which showed that an increase in Fe³⁺
490 concentration by 1×10^{-4} mol/L required the addition of 1.68×10^{-4} mol/L of the oxalate ion
491 concentration to provide sufficient free oxalate ions for REE precipitation [24].

492 Interestingly, an increase in ferric iron contamination also influences the precipitation of
493 other impurities, which results in higher purity for the rare earth product. This behavior was
494 observed while modeling the formation of calcium-oxalate monohydrate, which is the primary
495 precipitant, over a range of iron concentrations. The results in Figure 14 indicate a substantial
496 decrease in calcium precipitation from approximately 92% to 32% at pH 1.5 when iron
497 contamination increases from 150 ppm to 950 ppm. This adverse impact on calcium precipitation
498 is because of the reduced availability of oxalate anions at higher iron concentrations.

499

500

501

502

503

504

505

506

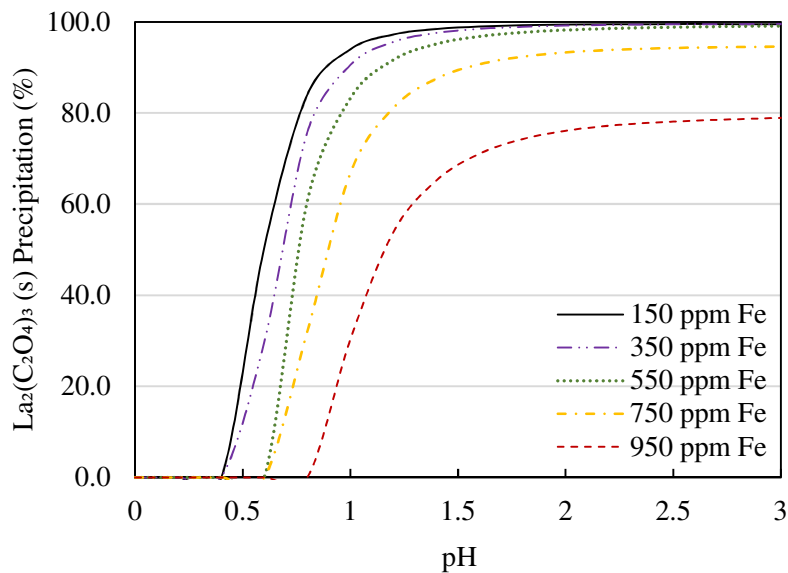
507

508

Table 8. The percentage distribution of oxalate species in the system with various amounts of Fe(III).

Oxalate Species	% of total concentration				
	150 ppm Fe ³⁺	350 ppm Fe ³⁺	550 ppm Fe ³⁺	750 ppm Fe ³⁺	950 ppm Fe ³⁺
C ₂ O ₄ ²⁻	0.135	0.077	0.036	0.016	0.000
Fe-C ₂ O ₄ ⁺	0.053	0.314	1.533	5.462	14.012
H ₂ -C ₂ O ₄	16.586	9.370	4.383	2.015	0.962
H-C ₂ O ₄ ⁻	38.306	21.770	10.191	4.680	2.230
La-C ₂ O ₄ ⁺	0.006	0.009	0.013	0.018	0.027
AlH-C ₂ O ₄ ²⁺	0.015	0.029	0.060	0.101	0.133
Al-(C ₂ O ₄) ₃ ³⁻	6.589	4.240	1.913	0.671	0.201
Al-(C ₂ O ₄) ₂ ⁻	7.421	8.137	7.805	6.004	3.795
Al-C ₂ O ₄ ⁺	0.429	0.832	1.705	2.854	3.781
Fe-(C ₂ O ₄) ₃ ³⁻	17.100	33.523	35.938	26.822	15.489
Fe-(C ₂ O ₄) ₂ ⁻	3.842	12.836	29.251	47.898	58.630
% Dissolved Oxalate	90.484	91.138	92.828	96.542	99.259
Dissolved Oxalate (M)	0.032	0.032	0.032	0.034	0.035
La ₂ (C ₂ O ₄) ₃ (s)	1.065	1.057	1.029	0.952	0.741
Ca-C ₂ O ₄ ·H ₂ O(s)	8.451	7.805	6.143	2.506	0.000
% Precipitated Oxalate	9.516	8.862	7.172	3.458	0.741
Precipitated Oxalate (M)	0.003	0.003	0.003	0.001	0.000

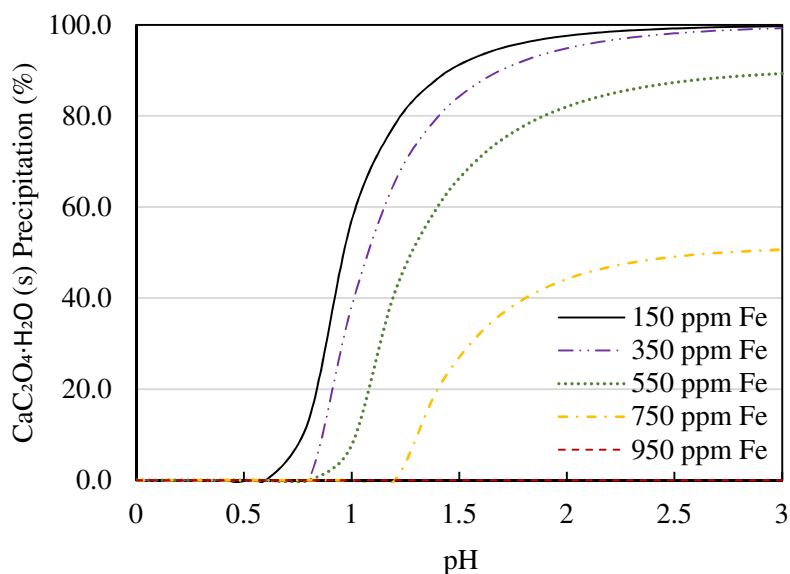
510



511

512 Figure 13. Effect of Fe concentration on La oxalate precipitation pH and efficiency. (0.035M C₂O₄²⁻,
 513 0.1M Cl⁻, 60 ppm Al³⁺, 130 ppm Ca²⁺, and 35 ppm La³⁺ at 25 °C calculated using Visual MINTEQ
 514 software).

515



516

517 Figure 14. Effect of Fe concentration on Ca oxalate precipitation pH and efficiency. (0.035M $C_2O_4^{2-}$,
 518 0.1M Cl^- , 150 ppm Fe^{3+} , 60 ppm Al^{3+} , 130 ppm Ca^{2+} , and 35 ppm La^{3+} at 25 °C simulated using Visual
 519 MINTEQ software.)

520

521 4. Conclusion:

522 This investigation was focused on the impact of oxalic acid dosage, iron contamination,
 523 pH, and temperature on the REE precipitation efficiency from a leachate generated from the mine
 524 waste material that contained relatively low concentrations of REEs and high concentrations of
 525 contaminants, i.e., Fe and Ca. A central composite design (CCD) was utilized to design the
 526 experimental program and analyze the data using Design-Expert software. The reaction kinetics
 527 data collected in this study indicated that the solution reaches an equilibrium state within five
 528 minutes following the start of the reaction. A quadratic model was developed using the
 529 experimental data and validated within the parameter range. The model was found to provide a
 530 good prediction of the parameter value effects as indicated by an adjusted R^2 value of 80%.

531 The results of the parametric study showed that all of the factors evaluated in this study
 532 have a significant impact on the REE precipitation efficiency. The oxalic acid concentration has a
 533 positive association with the REE precipitation efficiency, whereas the Fe contamination has a
 534 negative impact. Additionally, increasing the pH of the reaction promoted the REE precipitation
 535 efficiency. Increasing the temperature of the solution provided a negative effect on the REE
 536 precipitation efficiency, which indicated that the REE oxalate precipitation is an exothermic
 537 reaction.

538 The response surface quantified the interaction effect between oxalic acid dosage and Fe
 539 contamination on REE precipitation efficiency. With low Fe contamination in solution, the oxalic
 540 acid concentration required to achieve 95% REE precipitation is less than 80g/L at a dosage of 40
 541 ml/L. A further increase in the oxalic acid concentration to 160g/L did not impact the REE

542 precipitation efficiency. When the Fe(III) concentration in solution was elevated, the REE
543 precipitation efficiency reduced dramatically due to the complexation between the oxalate anions
544 and Fe(III). The speciation study showed that, with low rare earth concentrations in solution, the
545 RE oxalate precipitation is incomplete even in the presence of excess oxalate ions. In addition, the
546 Fe concentration has a significant impact on oxalate species distribution in solution at equilibrium.
547 Consequently, the precipitation pH of the rare earth oxalate shifted to a higher pH range.
548 Interestingly, the presence of Fe in the solution reduced the precipitation of other contaminant
549 ions, i.e., calcium oxalate, due to the occupation of the oxalate ions. With increasing Fe
550 concentration in solution, the precipitation efficiency of calcium oxalate is reduced more than the
551 rare earth oxalate.

552 This paper presented a model that effectively predicts the oxalic acid dosage needed at different
553 pH to achieve a desirable REE precipitation efficiency from a solution with various Fe
554 concentrations. It can be concluded from this investigation that reducing the concentration of
555 contaminants like Fe in the solution is essential to achieve high REE precipitation efficiency and
556 a reduction in oxalic acid consumption.

557

558

559 **Acknowledgement:** This material is based upon work supported by the Department of Energy
560 Award Number DE-FE0031827.

561 **Disclaimer:** This report was prepared as an account of work sponsored by an agency of the United
562 States Government. Neither the United States Government nor any agency thereof, nor any of their
563 employees, makes any warranty, express or implied, or assumes any legal liability or responsibility
564 for the accuracy, completeness, or usefulness of any information, apparatus, product, or process
565 disclosed, or represents that its use would not infringe privately owned rights. Reference herein to
566 any specific commercial product, process, or service by trade name, trademark, manufacturer, or
567 otherwise does not necessarily constitute or imply its endorsement, recommendation, or favoring
568 by the United States Government or any agency thereof. The views and opinions of authors
569 expressed herein do not necessarily state or reflect those of the United States Government or any
570 agency thereof.

571

572 **References**

- 573 [1] G. Tyler, "Rare earth elements in soil and plant systems - A review," *Plant and Soil*, vol.
574 267, no. 1–2. Springer Netherlands, pp. 191–206, Dec. 2004, doi: 10.1007/s11104-005-
575 4888-2.
- 576 [2] R. Chi and D. Wang, "Beneficiation and Extraction of Rare Earth Ore," 1996.
- 577 [3] Y. Kanazawa and M. Kamitani, "Rare earth minerals and resources in the world," *J. Alloys*
578 *Compd.*, vol. 408, pp. 1339–1343, 2006, doi: 10.1016/j.jallcom.2005.04.033.
- 579 [4] T. Dutta *et al.*, "Global demand for rare earth resources and strategies for green mining,"
580 *Environmental Research*, vol. 150. Academic Press Inc., pp. 182–190, Oct. 2016, doi:
581 10.1016/j.envres.2016.05.052.
- 582 [5] Z. Chen, "Global rare earth resources and scenarios of future rare earth industry," *J. Rare*
583 *Earths*, vol. 29, no. 1, pp. 1–6, 2011, doi: 10.1016/S1002-0721(10)60401-2.
- 584 [6] E. Alonso *et al.*, "Evaluating rare earth element availability: A case with revolutionary
585 demand from clean technologies," *Environ. Sci. Technol.*, vol. 46, no. 6, pp. 3406–3414,
586 Mar. 2012, doi: 10.1021/es203518d.
- 587 [7] V. V. Seregin, S. Dai, Y. Sun, and I. Y. Chekryzhov, "Coal deposits as promising sources
588 of rare metals for alternative power and energy-efficient technologies," *Applied*
589 *Geochemistry*, vol. 31. Pergamon, pp. 1–11, Apr. 2013, doi:
590 10.1016/j.apgeochem.2013.01.009.
- 591 [8] V. G. Papangelakis and G. Moldoveanu, "Recovery of Rare Earth Elements From Clay
592 Minerals," *1St Eur. Rare Earth Resour. Conf.*, pp. 191–202, 2014.
- 593 [9] R. Chi, J. Xu, P. He, Y. Z.-T. of the N. M. S. of China, and undefined 1995, "Recovering
594 RE from leaching liquor of rare earth ore by extraction."
- 595 [10] Mark Lawrence Strauss, "Investigation into the Separation and Purification of Europium
596 and Yttrium Oxides from Waste Fluorescent Lamps," 2018.
- 597 [11] M. L. Strauss, "The recovery of rare earth oxides from waste fluorescent lamps," 2016.
- 598 [12] R. G. Silva, C. A. Morais, L. V. Teixeira, and É. D. Oliveira, "Selective Precipitation of
599 High-Quality Rare Earth Oxalates or Carbonates from a Purified Sulfuric Liquor Containing
600 Soluble Impurities," *Mining, Metallurgy and Exploration*, vol. 36, no. 5. Springer, pp. 967–
601 977, Oct. 2019, doi: 10.1007/s42461-019-0090-6.
- 602 [13] D. Beltrami, G. J-P Deblonde, S. Bélair, and V. Weigel, "Lawrence berkeley national
603 laboratory recent work title recovery of yttrium and lanthanides from sulfate solutions with
604 high concentration of iron and low rare earth content Publication Date Recovery of yttrium
605 and lanthanides from sulfate solutions with," *Elsevier*, 2015, doi:
606 10.1016/j.hydromet.2015.07.015.
- 607 [14] D.-Y. Chung, E.-H. Kim, E.-H. Lee, and J.-H. Yoo, "Solubility of rare earth oxalate in
608 oxalic and nitric acid media," *J. Ind. Eng. Chem.*, vol. 4, no. 4, pp. 277–284, 1998.
- 609 [15] J. S. Kim, H. S. Kim, M. J. Kim, J.-Y. Lee, and J. R. Kumar, "Status of separation and

- 610 purification of rare earth elements from Korean ore,” in *Rare Metal Technology 2015*,
611 Springer, 2015, pp. 117–126.
- 612 [16] K. N. Han, “Characteristics of precipitation of rare earth elements with various
613 precipitants,” *Minerals*, vol. 10, no. 2, 2020, doi: 10.3390/min10020178.
- 614 [17] R. Bautista and M. W. Vegas, “Rare Earths: Extraction, Preparation and Applications.”
- 615 [18] R. Chi and Z. Xu, “A solution chemistry approach to the study of rare earth element
616 precipitation by oxalic acid,” *Metall. Mater. Trans. B*, vol. 30, no. 2, pp. 189–195, 1999,
617 doi: 10.1007/s11663-999-0047-0.
- 618 [19] M. Woyski and R. H. Chemistry, “The rare earths and rare earth compounds,” *Intersci. Pub.*
619 *NY*.
- 620 [20] K. N. Han, “Effect of anions on the solubility of rare earth element-bearing minerals in
621 acids,” *Mining, Metall. Explor.*, vol. 36, no. 1, pp. 215–225, 2019.
- 622 [21] K. N. Han, J. J. Kellar, W. M. Cross, and S. Safarzadeh, “Opportunities and challenges for
623 treating rare-earth elements,” *Geosystem Eng.*, vol. 17, no. 3, pp. 178–194, 2014.
- 624 [22] H. Güneş, H. E. Obuz, and M. Alkan, “Selective Precipitation of Th and Rare-Earth
625 Elements from HCl Leach Liquor,” in *Minerals, Metals and Materials Series*, 2019, pp. 81–
626 86, doi: 10.1007/978-3-030-05740-4_9.
- 627 [23] I. Bureau, “(12) INTERNATIONAL APPLICATION PUBLISHED UNDER THE
628 PATENT COOPERATION TREATY (PCT) (19) World Intellectual Property Organization
629 RIGHT OF CANADA AS REPRESENTED BY THE MINISTER OF NATURAL
630 RESOURCES,” Apr. 2017.
- 631 [24] W. Zhang, A. Noble, B. Ji, and Q. Li, “Effects of contaminant metal ions on precipitation
632 recovery of rare earth elements using oxalic acid,” *J. Rare Earths*, Nov. 2020, doi:
633 10.1016/j.jre.2020.11.008.
- 634 [25] H. Watts and Y.-K. Leong, “Predicting the Logarithmic Distribution Factors for
635 Coprecipitation into an Organic Salt: Selection of Rare Earths into a Mixed Oxalate,”
636 *Minerals*, vol. 10, no. 8, p. 712, Aug. 2020, doi: 10.3390/min10080712.
- 637 [26] C. He, E. Makovicky, and B. Øsbaeck, “Thermal stability and pozzolanic activity of calcined
638 illite,” *Appl. Clay Sci.*, vol. 9, no. 5, pp. 337–354, 1995.
- 639 [27] D. T. Erwin, D. J. Bennett, M. K. M. Gladden, and F. E. Cole, “A comparison of the Tiselius
640 risk index (Ri) and relative saturation (RS) of calcium oxalate (CaOx) in stone formers,” in
641 *Urolithiasis and Related Clinical Research*, Springer, 1985, pp. 769–771.
- 642 [28] D. Beltrami, G. J. P. Deblonde, S. Bélair, and V. Weigel, “Recovery of yttrium and
643 lanthanides from sulfate solutions with high concentration of iron and low rare earth
644 content,” *Hydrometallurgy*, vol. 157, no. October, pp. 356–362, 2015, doi:
645 10.1016/j.hydromet.2015.07.015.
- 646 [29] P. Josso, S. Roberts, D. A. H. Teagle, O. Pourret, R. Herrington, and C. Ponce de Leon
647 Albarran, “Extraction and separation of rare earth elements from hydrothermal

- 648 metalliferous sediments,” *Miner. Eng.*, vol. 118, pp. 106–121, Mar. 2018, doi:
649 10.1016/j.mineng.2017.12.014.
- 650 [30] X. Zeng, J. Li, and B. Shen, “Novel approach to recover cobalt and lithium from spent
651 lithium-ion battery using oxalic acid,” *J. Hazard. Mater.*, vol. 295, pp. 112–118, Sep. 2015,
652 doi: 10.1016/j.jhazmat.2015.02.064.
- 653 [31] L. Sun and K. Qiu, “Organic oxalate as leachant and precipitant for the recovery of valuable
654 metals from spent lithium-ion batteries,” *Waste Manag.*, vol. 32, no. 8, pp. 1575–1582, Aug.
655 2012, doi: 10.1016/j.wasman.2012.03.027.
- 656 [32] D. Papias, M. Taxiarchou, I. Paspaliaris, and A. Kontopoulos, “Mechanisms of dissolution
657 of iron oxides in aqueous oxalic acid solutions,” *Hydrometallurgy*, vol. 42, no. 2, pp. 257–
658 265, Sep. 1996, doi: 10.1016/0304-386X(95)00104-O.
- 659 [33] Z. A. Sari, M. D. Turan, H. Nizamoğlu, A. Demiraslan, and T. Depci, “Selective Copper
660 Recovery with HCl Leaching from Copper Oxalate Material,” *Mining, Metall. Explor.*, vol.
661 37, no. 3, pp. 887–897, Jun. 2020, doi: 10.1007/s42461-020-00196-8.
- 662 [34] E. Christodoulou, D. Papias, and I. Paspaliaris, “Calculated solubility of trivalent iron and
663 aluminum in oxalic acid solutions at 25 °C,” *Can. Metall. Q.*, vol. 40, no. 4, pp. 421–432,
664 2001, doi: 10.1179/cm.2001.40.4.421.
- 665 [35] M. A. R. Önal, C. R. Borra, M. Guo, B. Blanpain, and T. Van Gerven, “Recycling of NdFeB
666 Magnets Using Sulfation, Selective Roasting, and Water Leaching,” *J. Sustain. Metall.*, vol.
667 1, no. 3, pp. 199–215, Sep. 2015, doi: 10.1007/s40831-015-0021-9.
- 668 [36] Y. Yang, X. Wang, M. Wang, H. Wang, and P. Xian, “Recovery of iron from red mud by
669 selective leach with oxalic acid,” *Hydrometallurgy*, vol. 157, pp. 239–245, Oct. 2015, doi:
670 10.1016/j.hydromet.2015.08.021.
- 671 [37] F. Liu, Z. Liu, Y. Li, and B. Wilson, “Recovery and separation of gallium (III) and
672 germanium (IV) from zinc refinery residues: Part I: Leaching and iron (III) removal,”
673 *Elsevier*.
- 674 [38] P. Venkatesan, Z. H. I. Sun, J. Sietsma, and Y. Yang, “An environmentally friendly electro-
675 oxidative approach to recover valuable elements from NdFeB magnet waste,” *Sep. Purif.*
676 *Technol.*, vol. 191, pp. 384–391, 2018, doi: 10.1016/j.seppur.2017.09.053.
- 677 [39] A. Apelblat and E. Manzurola, “Solubility of oxalic, malonic, succinic, adipic, maleic,
678 malic, citric, and tartaric acids in water from 278.15 to 338.15 K,” *J. Chem. Thermodyn.*,
679 vol. 19, no. 3, pp. 317–320, Mar. 1987, doi: 10.1016/0021-9614(87)90139-X.
- 680 [40] S. T. Hussain and G. A. Khan, “Solubility of Oxalic Acid,” *Asian J. Res. Chem.*, vol. 5, no.
681 11, pp. 1323–1330, 2012.
- 682 [41] *CRC Handbook of Chemistry and Physics*, 66th ed. Boca Raton, FL: CRC Press Inc, 1985.
- 683 [42] A. Bard, R. Parsons, and J. Jordan, “Standard potentials in aqueous solution,” 1985.
- 684
- 685